

Gigahertz modulation of tunable terahertz radiation from photomixers driven at telecom wavelengths

M. Martin,¹ J. Mangeney,^{1,a)} P. Crozat,¹ Y. Chassagneux,¹ R. Colombelli,¹ N. Zerounian,¹ L. Vivien,¹ and K. Blary²

¹Institut d'Electronique Fondamentale, CNRS UMR 8622, Univ Paris-Sud, 91405 Orsay Cedex, France

²Institut d'Electronique de Microélectronique et de Nanotechnologie, CNRS UMR 8520, Cité Scientifique, 59652 Villeneuve d'Ascq Cedex, France

(Received 31 August 2008; accepted 9 September 2008; published online 3 October 2008)

Here, we report the gigahertz-rate modulation of a tunable terahertz carrier. Terahertz radiation, tunable from 300 GHz to 1.2 THz, is generated by mixing two telecom lasers with an offset frequency in an ultrafast $\text{In}_{0.53}\text{Ga}_{0.47}\text{As}$ photoconductive device coupled to a broadband antenna. The microwave modulation applied to the telecom lasers is directly transferred to the terahertz carrier. A maximum modulation rate of 20 GHz has been achieved, and the bandwidth is independent of the carrier frequency. © 2008 American Institute of Physics.

[DOI: 10.1063/1.2993352]

Wireless data transmission systems are enjoying a rapid diffusion and development, in order to support the communication needs of our society. Bluetooth, Wi-Fi and Wi-Max are some well-known examples, all operating at gigahertz carrier frequencies. The increase in data rate transmission, with the objective of attaining the capabilities of fiber-linked optical communication systems, is a particularly important research area. For instance, a subterahertz wireless link has recently been developed by Hirata *et al.*¹ for data transmission at 10 Gbit/s, the data rate per channel of current high-speed optical networks. However, optical networks bandwidths of 40, 80, and even 160 GHz will possibly be needed in the near future. To support these high data rates, carrier frequencies for wireless communication networks in the terahertz frequency range will be an almost forced choice.² This is a major challenge since terahertz photonics is still in its infancy, with several scientific and engineering problems to be solved. For instance, the technology of choice to encode high-frequency data signals onto a terahertz carrier is still an open issue.³⁻⁵ In this letter, we demonstrate that the high-speed modulation of two telecom lasers can be directly transferred onto a cw terahertz carrier frequency generated by the lasers themselves, via a photomixing process in an ultrafast $\text{In}_{0.53}\text{Ga}_{0.47}\text{As}$ photomixer. The maximum modulation rate of 20 GHz achieved is only limited by the bandwidth of the optical modulator used. In addition, the terahertz carrier frequency can be easily tuned by changing the wavelength of one telecom laser. This is a crucial feature for free space communications. It allows one to match one of the atmospheric transparency frequency windows located between 300 GHz and 1 THz.

The experimental system uses two cw laser diodes operating at $\lambda_{\text{laser}} \approx 1.55 \mu\text{m}$, and one of the lasers is frequency tunable in 12.5 MHz steps. The two telecom lasers are then amplitude modulated at gigahertz rates with a lithium niobate Mach-Zehnder modulator. After amplification in an erbium-doped amplifier, the fiber output is focused onto an interdigitated photomixer made from an ion-irradiated $\text{In}_{0.53}\text{Ga}_{0.47}\text{As}$ photoconductive layer, operating at room

temperature.⁶ The ac current generated by the photomixer feeds the dipole-spiral antenna of the device, which is coupled to free space via a hemispherical Si lens. Two time constants characterize the device, the electron lifetime (0.86 ps) (Ref. 6) and the $R_A C$ time constant, evaluated to 0.124 ps from antenna geometry. The photomixer, when it is pumped with 40 mW total optical power and biased at 1.5 V, typically delivers 45 and 10 nW of power at 0.5 and 1 THz, respectively. The cw terahertz emission generated by the photomixer is then collimated by a parabolic mirror and fed into a Fourier transform infrared (FTIR) spectrometer. A poly-tetrafluoro-ethylene plate is placed in front of the FTIR to block out the $\lambda = 1.55 \mu\text{m}$ laser light and also to allow one to operate the system under vacuum to eliminate air or water absorption. The detector used is a liquid-He-cooled 3 mm diameter Si bolometer.

Continuous tunability of the terahertz carrier, within the spectral response of the photomixing module, can be achieved by tuning the wavelength of one of the two lasers. Figure 1 shows the normalized spectra of the photomixer terahertz output under illumination by the two cw telecom lasers. Several frequency offsets have been used. The maxi-

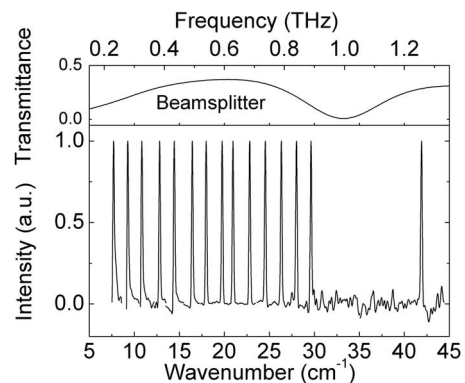


FIG. 1. Normalized FTIR spectra of terahertz waves emitted by the $\text{In}_{0.53}\text{Ga}_{0.47}\text{As}$ based photomixer illuminated by two cw telecom lasers. The gap observed between 0.9 and 1.2 THz is due to the low transparency in this spectral region of the 100- μm -thick Mylar beamsplitter used in the FTIR spectrometer (transmission in inset). The FTIR was operated in rapid scan mode.

^{a)}Electronic mail: juliette.mangeney@ief.u-psud.fr.

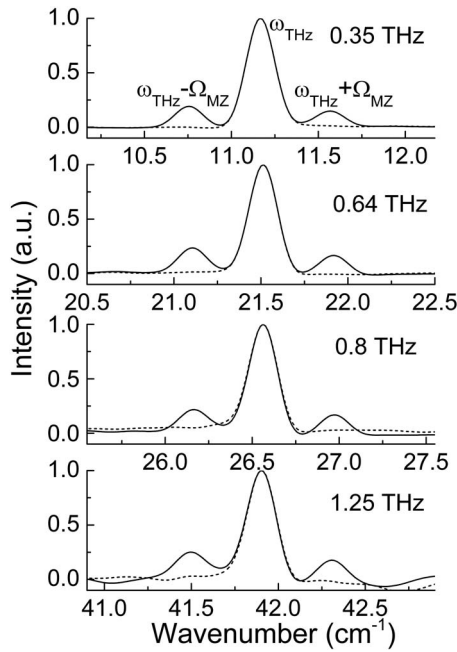


FIG. 2. Normalized FTIR spectra of the photomixer output when the device is illuminated by the two telecom lasers modulated in amplitude. Several frequency offsets corresponding to $\omega_{\text{THz}}=0.35, 0.64, 0.8,$ and 1.25 THz are presented. Both the emissions with the high-frequency modulation on (plain curves) and off (dotted lines) are shown.

imum ω_{THz} detected is 1.22 THz. The optical modulator is not present for this set of experiments. The spectral position of the terahertz emission is in agreement with the frequency difference of the telecom lasers, which is fixed for each measurement and determined with an optical spectrum analyzer. When an amplitude modulation is applied to the two driving telecom lasers, the photomixer emission spectrum is modified. The corresponding terahertz spectra are shown in Fig. 2 (plain lines), for $\omega_{\text{THz}}=0.35$ THz to $\omega_{\text{THz}}=1.25$ THz. The two telecom lasers illuminating the device are modulated at a microwave frequency, $\Omega=12.2$ GHz. The extinction ratio, defined as the ratio between the maximum and the minimum intensities of the modulating lasers, is $X=6$. The signature of transfer of the microwave modulation of the driving lasers onto the terahertz carrier is the appearance of microwave shifts (or sidebands) at $\omega=\omega_{\text{THz}}+\Omega$ and $\omega=\omega_{\text{THz}}-\Omega$ (plain curves in Fig. 1). In Fig. 2, dotted lines illustrate the spectra exhibiting only the carrier frequency ω_{THz} when no modulation is applied. The relative heights of the lower and upper sidebands are 0.19 (within 7% variation) and 0.16 (within 15% variation), respectively, for all the tested carrier frequencies ω_{THz} . These measurements demonstrate the transfer of >10 GHz modulation from an optical telecom carrier to a free space terahertz carrier, with a transfer efficiency that remains essentially constant in the 0.35–1.25 THz range. Note that the origin of the slight height difference between the two sidebands is unclear yet. It could be partially attributed to the limited spectral resolution of our FTIR. Indeed, the instrument resolution of 0.12 cm^{-1} , which corresponds to a frequency resolution of 3.6 GHz, is significantly lower than the few megahertz widths of the lines.

Figure 3 shows spectra of the amplitude modulated terahertz radiation emitted by the photomixer for several values of the extinction ratio. The carrier frequency is set at $\omega_{\text{THz}}=0.66$ THz, and X ranges from 2 to 10. An increase in the

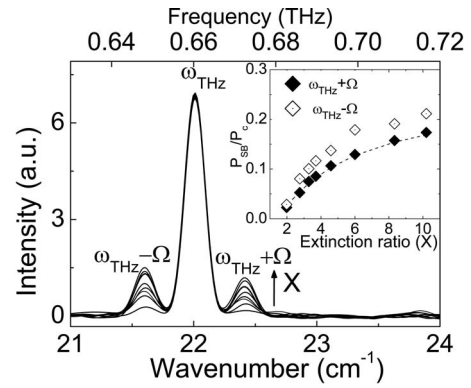


FIG. 3. FTIR spectra at several extinction ratios X for frequency offsets between the two modulated telecom lasers of 0.66 THz. Inset: Sideband power P_{SB} , normalized to the carrier power P_c , plotted as a function of the extinction ratio X . The filled and open diamonds represent the peak amplitudes at frequency $\omega_{\text{THz}}+\Omega$ and $\omega_{\text{THz}}-\Omega$, respectively. The dashed line indicates the theoretical law.

sideband power is clearly observable with increasing X , while the central line at frequency $\omega_{\text{THz}}=0.66$ THz remains unchanged as expected. In order to better understand the spectral shape of the generated terahertz radiation, we derived a simple analytical model of the amplitude modulated terahertz electric field using the photomixing theory⁷ and under the hypothesis that the optical modulator is operating in a linear regime. In this case, the amplitude modulated terahertz electric field can be expressed as follows:

$$E_{\text{THz}} = \frac{E_0}{2} \left\{ \cos(\omega_{\text{THz}}t) + \frac{1}{2}m[\cos(\omega_{\text{THz}}t - \Omega t) + \cos(\omega_{\text{THz}}t + \Omega t)] \right\}.$$

where m is the modulation coefficient defined by $m=X-1/X+1$. E_0 is the peak amplitude of the terahertz electric field generated by the photomixer in the absence of modulation. A Fourier transform is used to calculate the sideband power P_{SB} relative to the carrier power P_c : $P_{\text{SB}}/P_c = \frac{1}{4}(X-1/X+1)^2$. The experimental (diamond symbols) and calculated (dashed line) values of P_{SB} normalized to P_c are plotted as a function of X in inset of Fig. 3. Note that no adjustable parameter has been used in the calculation. The model explains very well the amplitude of the $\omega+\Omega$ peak, but predicts a $\omega-\Omega$ peak smaller than the observed one. The comparison between experimental data and theoretical prediction suggests that our simple model contains the main physical phenomena involved in the photomixer operation. The observed discrepancy between the lower sideband levels and the model may originate from a measurement problem, such as for instance the limited spectral resolution of the FTIR spectrometer. With this proviso, the physics of the modulation is well understood and it can be applied to engineering applications such as high-bit-rate wireless telecommunication systems.

The Fig. 4 shows microwave sidebands at several modulation frequencies from 8.1 to 20 GHz. The spectra are shown as frequency shifts relative to the 0.66 THz carrier. To take into account the decrease in the amplitude modulation of the two telecom lasers as the modulation frequency increases, the spectra plotted in Fig. 4 are normalized by the factor m^2 . This allows the relative heights of the sidebands to

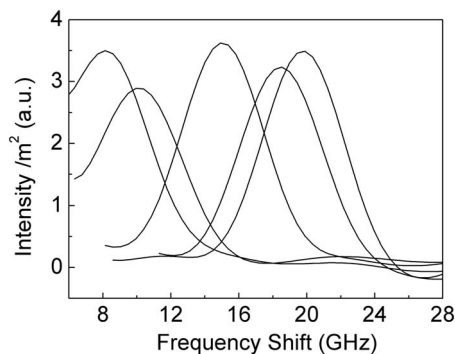


FIG. 4. Microwave sidebands at several modulation frequencies from 8.1 to 20 GHz. The -3 dB electro-optic bandwidth of the Mach-Zehnder modulator is 20 GHz. Spectra are shown as frequency shift relative to the 0.66 THz carrier and the amplitude are normalized by the factor m^2 .

be compared directly. One obvious feature of the data is that the sidebands do not decrease as the modulation frequency increases, and the transfer efficiency is preserved up to 20 GHz.

However, error-free data transmission over few hundreds of meters requires reasonably high output powers (of the order of ten microwatts²) for the terahertz carrier, with low noise characteristics of the transmitted signal. Currently photomixing devices driven at $\lambda \approx 1.55 \mu\text{m}$ are based on ion-irradiated $\text{In}_{0.53}\text{Ga}_{0.47}\text{As}$ photoconductive material, as well as on low temperature- $\text{In}_{0.53}\text{Ga}_{0.47}\text{As}$,⁸ $\text{ErAs}:\text{In}_{0.53}\text{Ga}_{0.47}\text{As}$ (Ref. 9) photoconductive materials, $\text{In}_{0.53}\text{Ga}_{0.47}\text{As}$ n - i - p - n - i - p superlattices,¹⁰ and untraveling photodiode.¹ All these technologies allow one to reach output powers in the tens of nanowatts range at 1 THz, except for the last one which can deliver $12.6 \mu\text{W}$ at a frequency 1.04 THz.² It is expected that the output power delivered by terahertz photomixers driven at $\lambda = 1.55 \mu\text{m}$ will increase in the near future, thanks to a combination of basic research and technological developments. Strategies currently pursued include design of antennas that ensure a better extraction of the terahertz waves,¹¹ traveling-wave scheme,¹² or ballistic transport¹⁰ to overcome the transit time versus RC time trade-off, the use of Fabry-Pérot cavity or three-dimensional photonic

crystal¹³ to enhance the carrier generation and collection, and substrate report to improved passive thermal sinking.

In conclusion, we have demonstrated the efficient transfer of a gigahertz modulation from an optical carrier at telecom wavelengths to a free space terahertz beam. The principle we have demonstrated is general and it can be applied to any photomixing process, regardless of its device implementation. Moreover, by illuminating the photomixing module by multimode laser, several terahertz single-frequency modes can be simultaneously emitted in applications including wavelength-division multiplexing.

The authors would like to thank C. Boukari from CSNSM in Orsay for ion irradiation and J. F. Lampin from IEMN for fruitful discussion. This work has been carried out in the frame of the french RTB network. R.C. acknowledges support from the EURYI scheme award.

¹A. Hirata, T. Kosugi, H. Takahashi, R. Yamaguchi, F. Nakajima, T. Furuta, H. Ito, H. Sugahara, Y. Sato, and T. Nagatsuma, *IEEE Trans. Microwave Theory Tech.* **54**, 1937 (2006).

²T. Kleine-Ostmann, P. Dawson, K. Piez, G. Hein, and M. Koch, *Appl. Phys. Lett.* **84**, 3555 (2004).

³S. Barbieri, W. S. Maineult, S. Dhillon, C. Sirtori, J. Alton, and N. Breuil, *Appl. Phys. Lett.* **91**, 143510 (2007).

⁴L. Fekete, F. Kadlec, P. Kužel, and H. Němec, *Opt. Lett.* **32**, 680 (2007).

⁵R.-T. Chen, W. J. Padilla, J. M. O. Zide, S. R. Bank, A. C. Gossard, A. J. Taylor, and R. D. Averitt, *Opt. Lett.* **32**, 1620 (2007).

⁶J. Mangeney, A. Merigault, N. Zerounian, P. Crozat, K. Blary, and J.-F. Lampin, *Appl. Phys. Lett.* **91**, 241102 (2007).

⁷E. R. Brown, *Int. J. High Speed Electron. Syst.* **13**, 497 (2003).

⁸C. Baker, I. S. Gregory, W. R. Tribe, E. H. Linfield, and M. Missous, *Opt. Express* **13**, 9639 (2005).

⁹M. Sukhotin, E. R. Brown, A. C. Gossard, D. Driscoll, M. Hanson, P. Maker, and R. Muller, *Appl. Phys. Lett.* **82**, 3116 (2003).

¹⁰S. Preu, F. H. Renner, S. Malzer, G. H. Döhler, L. J. Wang, M. Hanson, A. C. Gossard, T. L. J. Wilkinson, and E. R. Brown, *Appl. Phys. Lett.* **90**, 212115 (2007).

¹¹E. Peytavit, J.-F. Lampin, T. Akalin, and L. Desplanque, *Electron. Lett.* **43**, 73 (2007).

¹²S. Matsuura, G. A. Blake, R. A. Wyss, J. C. Pearson, C. Kadow, A. W. Jackson, and A. C. Gossard, *Appl. Phys. Lett.* **74**, 2872 (1999).

¹³M. Iida, M. Tani, P. Gu, K. Sakai, M. Watanabe, H. Kitahara, S. Kato, M. Suenaga, and H. Kondo, *Jpn. J. Appl. Phys., Part 2* **42**, L1442 (2003).